Computer Methods in Biomechanics and Biomedical Engineering
Publication details, including instructions for authors and subscription information:
http://www.tandfonline.com/loi/gcmb20

Biomechanical effect after Coflex and Coflex rivet implantation for segmental instability at surgical and adjacent segments: a finite element analysis

Cheng-Chan Lo [a] , Kai-Jow Tsai [b] , Shih-Hao Chen [c] , Zheng-Cheng Zhong [d] & Chinghua Hung [a]

[a] Department of Mechanical Engineering , National Chiao Tung University , 1001 Ta Hsueh Road, Hsinchu , Taiwan

[b] Department of Orthopaedic Surgery , Cathay General Hospital , Taipei , Taiwan

[c] Department of Orthopaedics , Tzu Chi General Hospital , Taichung , Taiwan

[d] Department of Physical Therapy and Assistive Technology , National Yang Ming University , 155, Section 2, Li-Nung Street, Taipei , Taiwan

Published online: 23 May 2011.

To cite this article: Cheng-Chan Lo , Kai-Jow Tsai , Shih-Hao Chen , Zheng-Cheng Zhong & Chinghua Hung (2011) Biomechanical effect after Coflex and Coflex rivet implantation for segmental instability at surgical and adjacent segments: a finite element analysis, Computer Methods in Biomechanics and Biomedical Engineering, 14:11, 969-978, DOI: 10.1080/10255842.2010.502894

To link to this article: http://dx.doi.org/10.1080/10255842.2010.502894

Computer Methods in Biomechanics and Biomedical Engineering
Vol. 14, No. 11, November 2011, 969–978

Taylor & Francis
Taylor & Francis Group

Biomechanical effect after Coflex and Coflex rivet implantation for segmental instability at surgical and adjacent segments: a finite element analysis

Cheng-Chan Lo[a], Kai-Jow Tsai[b], Shih-Hao Chen[c], Zheng-Cheng Zhong[d] and Chinghua Hung[a]*

[a]*Department of Mechanical Engineering, National Chiao Tung University, 1001 Ta Hsueh Road, Hsinchu, Taiwan*
[b]*Department of Orthopaedic Surgery, Cathay General Hospital, Taipei, Taiwan;* [c]*Department of Orthopaedics, Tzu Chi General Hospital, Taichung, Taiwan;* [d]*Department of Physical Therapy and Assistive Technology, National Yang Ming University, 155, Section 2, Li-Nung Street, Taipei, Taiwan*

(*Received 12 November 2009; final version received 17 June 2010*)

The Coflex device may provide stability to the surgical segment in extension but does not restore stability in other motion. Recently, a modified version called the Coflex rivet has been developed. The effects of Coflex and Coflex rivet implantation on the adjacent segments are still not clear; therefore, the purpose of this study was to investigate the biomechanical differences between Coflex and Coflex rivet implantation by using finite element analyses. The results show that the Coflex implantation can provide stability in extension, lateral bending, and axial rotation at the surgical segment, and it had no influence at adjacent segments except for extension. The Coflex rivet implantation can provide stability in all motions and reduce disc annulus stress at the surgical segment. Therefore, the higher range of motion and stress induced by the Coflex rivet at both adjacent discs may result in adjacent segment degeneration in flexion and extension.

Keywords: lumbar spinal stenosis; interspinous process device; Coflex rivet follower load; disc annulus stress; finite element analysis

1. Introduction

Lumbar spinal stenosis (LSS) is a common disabling disease in the elderly. The reduced disc height narrows the spinal canal and the neural foramina, eventually resulting in nerve compression (Arbit and Pannullo 2001). The symptoms of LSS include bilateral radicular pain and intermittent neurogenic claudication, sensation disturbance and loss of muscle strength in the legs. Many surgeons perform decompression for spinal stenosis and reconstruct the segment with rigid fusion devices. However, rigid fusion may cause increased stress at the adjacent discs, resulting in degeneration of adjacent segments (Kuslich et al. 2000; Lai et al. 2004; Zucherman et al. 2004). Therefore, flexible nonfusion devices such as the interspinous process device were developed with the intention of reducing adjacent segment degeneration.

An interspinous process device is defined as a flexible system that can preserve spinal movement and improve load transmission of spinal motion segments through the non-fusion technique (Sengupta 2004; Christie et al. 2005). There have been a number of interspinous process devices such as Coflex, Wallis, Diam and X-Stop, tested for treating LSS with different biomechanical designs. The Coflex (Paradigm Spine, Wurmlingen, Germany) was originally developed as an interspinous U-shaped device and is placed between two adjacent spinous processes (Kaech et al. 2002; Cho 2005; Eif and Schenke 2005). After implantation, the lateral wings are crimped towards the spinous processes to improve fixation. The U-shaped structure is designed to allow the lumbar spine to have controlled movement in forward and backward bending. To improve stability in all motions, a modified version called the Coflex rivet has also been developed (Kettler et al. 2008), which adds two rivets to the Coflex.

Recently, many studies have evaluated the biomechanical behaviours of the Coflex and Coflex rivet devices. Tsai et al. (2006) used cadaveric lumbar L4 and L5 segments with implanted Coflex device to examine their biomechanical behaviour, and the results showed that the implanted Coflex device can provide stability for the lumbar spine in flexion–extension and axial rotation, except in lateral bending. Kong et al. (2007) reported 1-year follow-up outcomes after Coflex device implantation and traditional fusion for degenerative spinal stenosis. The results indicated that both the Coflex device and traditional fusion reduced the range of motion (ROM) at the surgical segment, but fewer effects were found at the adjacent segments with the Coflex device when compared with the increasing ROM with traditional fusion. Kettler et al. (2008) compared the Coflex and Coflex rivet devices using biomechanical experiments and found that both implants had strong stability in extension. However, the Coflex implant could not compensate the instability in flexion, lateral bending and axial rotation as well as the

*Corresponding author. Email: chhung@mail.nctu.edu.tw

ISSN 1025-5842 print/ISSN 1476-8259 online

http://dx.doi.org/10.1080/10255842.2010.502894
http://www.tandfonline.com

Coflex rivet did. Wilke et al. (2008) examined the biomechanical effects of different interspinous process devices for flexibility. The Coflex device had the best stabilising effect in extension, but poor stability in flexion. In lateral bending and axial rotation, the Coflex device had neither a stabilising nor a destabilising effect. Inconsistent results regarding the biomechanical effects of the Coflex device have been shown in previous studies. In addition, these studies are mostly a short-segment analysis focused on the surgical segment. The effect of the Coflex device and the Coflex rivet implantation on adjacent segments is still not clear.

Therefore, the purpose of this study was to investigate the biomechanical differences between the Coflex device and the Coflex rivet at surgical and adjacent segments by using finite element (FE) analyses on a five-segment spinal model. In addition, the study also compared these two interspinous process implantations with pedicle screw fixation. The main variables in the study include the ROM of spinal segments, the maximal von Mises stress at the disc annulus and the von Mises stress distribution at the surgical disc annulus.

2. Materials and methods

2.1 FE model of intact lumbar spine (intact model)

A validated 3D FE model of the intact lumbar spine was used. To create this model, computed tomography scans of the L1–L5 lumbar spine of a middle-aged healthy man were obtained at 1-mm intervals. The commercially available FE program, ANSYS 9.0 (ANSYS Inc., Canonsburg, PA, USA), was used to model the spinal segments. The FE model of the osseoligamentous lumbar spine included the vertebrae, intervertebral discs, endplates, posterior elements and the following ligaments: supraspinous, interspinous, ligamentum flavum, transverse, posterior longitudinal, anterior longitudinal and capsular. The material properties of the lumbar spine were assumed to be homogeneous, and a detailed description has been presented in our previous studies (Chen et al. 2009; Zhong et al. 2009). The ligaments were simulated using two-node link elements with tension resistance only, and the elements were arranged in the anatomic orientation. Eight-node solid elements were used for modelling of the cortical bone, cancellous bone, endplate, posterior bony structure and discs. The disc annulus consisted of fibres embedded in the ground substance. Annular fibres in 12 layers were modelled using two-node link elements with tension resistance only and placed in an anatomic orientation (Eberlein et al. 2001; Vena et al. 2005; Schmidt et al. 2006). The facet joints were treated as nonlinear 3D contact pairs using surface-to-surface contact elements, and the coefficient of friction was set to 0.1 (Chen et al. 2009; Zhong et al. 2009). The intact model consisted of 111,990 elements and 94,162 nodes (Figure 1(A)).

2.2 FE model of Coflex device implanted into the L3–L4 segment (Coflex model)

This model was a defect model implanted with the Coflex device at the L3–L4 segment. The defect model was used to simulate instability by cutting the ligamentum flavum, the facet capsules and 50% of the inferior bony facet bilaterally at the L3–L4 segment (Tsai et al. 2006; Kettler et al. 2008). In addition, the supraspinous ligaments and interspinous ligaments had to be resected before insertion.

The Coflex device is available in five sizes from 8 mm through 16 mm in 2 mm increments. The most suitable size of the Coflex device was chosen based on the patient's lumbar spine. In this study, a height of 14 mm was the best fit to our FE model. The geometry of the Coflex device was recreated by CAD software from the real product and then transferred into the ANSYS software to construct

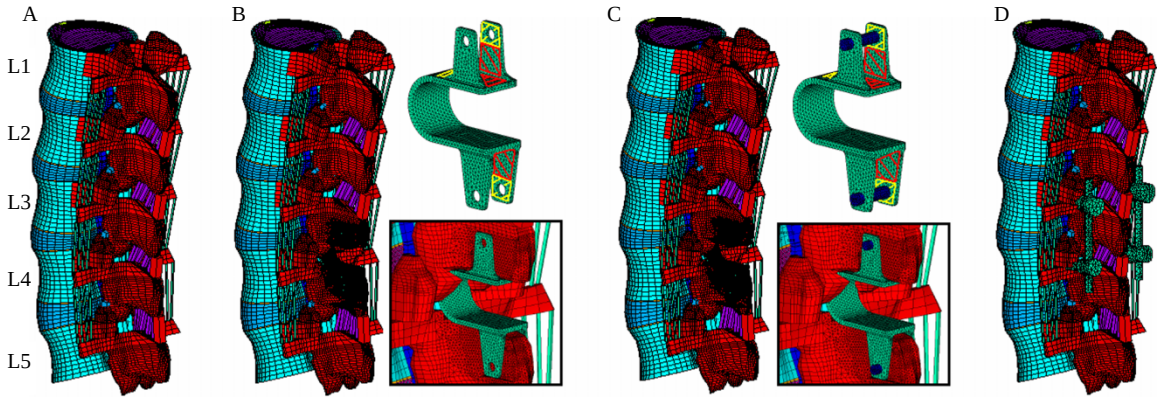

Figure 1. FE models of the L1–L5 lumbar spine: (A) intact model; (B) defect lumbar spine with Coflex inserted at the L3–L4 segment (Coflex model); (C) defect lumbar spine with Coflex rivet inserted at the L3–L4 segment (Coflex rivet model) and (D) defect lumbar spine with pedicle screws inserted at the L3–L4 segment (pedicle screw fixation model).

the Coflex FE model. To implant the Coflex device (Figure 1(B)), part of the L3–L4 interspinous process was removed to provide sufficient space into which the Coflex could be placed between the interspinous processes. The surface between the spinous processes and the wings of the Coflex was modelled as a surface-to-surface contact. The effect of teeth on the wings of the Coflex device was simplified by assigning a higher coefficient of friction (0.8) to the wing contact area (Figure 1(B), yellow region), and the coefficient of friction for the rest of the contact regions was set to 0.1 (Figure 1(B), red region). The higher coefficient of friction (0.8) was used in the contact interface to prevent device slip motion (Polikeit et al. 2003). The material used for the Coflex device was Ti-6Al-4V alloy. Young's modulus and Poisson's ratio were, respectively, assigned to be 113 GPa and 0.3.

2.3 FE model of Coflex rivet implanted into the L3–L4 segment (Coflex rivet model)

This model was a defect model implanted with the Coflex rivet device at the L3–L4 segment. The defect model was used to simulate instability by cutting the ligamentum flavum, the facet capsules and 50% of the inferior bony facet bilaterally at the L3–L4 segment (Tsai et al. 2006; Kettler et al. 2008). In addition, the supraspinous ligaments and interspinous ligaments had to be resected before insertion.

The Coflex rivet differs from the original Coflex implant by adding two rivets joining the wings and spinous processes (Figure 1(C)). The effect of the teeth on the wings of the Coflex rivet was also simplified by assigning a higher coefficient of friction (0.8) to the wing contact area (Figure 1(C), yellow region), and the coefficient of friction for the rest of the contact regions was set to 0.1 (Figure 1(C), red region). The rivets were simplified as cylinders and were constrained to both the holes on the wings of the Coflex and the spinous processes in all degrees of freedom (the degrees of freedom of screw nodes are interpolated with the corresponding degrees of freedom of the nodes on the Coflex and spinous processes during the execution of ANSYS program). The material used for the Coflex rivet was a Ti-6Al-4V alloy. The Young's modulus and Poisson's ratio, respectively, were assigned to be 113 GPa and 0.3, respectively.

2.4 FE model of bilateral pedicle screw fixation implanted into the L3–L4 segment (Pedicle screw fixation model)

This model was a defect model implanted with pedicle screw fixation at the L3–L4 segment. The difference between the pedicle screw fixation model and the above-mentioned implantation models was that the pedicle screw fixation model preserved the supraspinous ligaments and interspinous ligaments (Figure 1(D)). The pedicle screw fixation consisted of two rods (diameter, 4.5 mm) and four pedicle screws (diameter, 6 mm). The pedicle screws were inserted through the pedicles of the L3 and L4 vertebrae bilaterally. The pedicle screws were simplified as cylinders. The screw-bone interfaces were assigned to be fully constrained. The material used for the pedicle screws was Ti-6Al-4V. Young's modulus and Poisson's ratio were assigned to be 113 GPa and 0.3, respectively.

2.5 Boundary and loading conditions

For the preload method, traditional vertical preloads are unable to support the kinematic study of long lumbar spine specimens under higher physiologic compressive loads because the spine without active musculature buckles with just 120 N of vertical preload. In this study, the follower load concept was adopted and simulated at each motion segment in the model through the use of two-node thermal link elements. A 400-N compressive follower load was applied to each motion segment through induced contraction in these link elements by decreasing the temperature (Patwardhan et al. 2003; Panjabi et al. 2007). The link elements were attached near the centre of each vertebral body such that each element spanned the midplane of the discs. With these arrangements, a nearly ideal follower load path that remains tangential to the spinal curvature was constructed, and each spinal segment could be loaded in nearly pure compression without artefact motions.

A 10-Nm moment was applied to the intact model to mimic physiological motion (Yamamoto et al. 1989). In those motions, the multilevel lumbar spine was subjected to a maximal possible load without causing spinal injury. The other implanted models to be compared were also subjected to specific moments that produced overall motions that were equal to those of the intact model, using a hybrid test method (Panjabi 2007; Zhong et al. 2009). The detailed total lumbar ROMs of the intact model under the hybrid test method were 16.37° in flexion, 10.75° in extension, 15.27° in right lateral bending and 8.44° in right axial rotation. These ROMs were a baseline with which the total lumbar motion among the intact and implantation models under the hybrid test method could be matched (Table 1). The resulting deviation of ROMs among the three FE models was controlled within 0.64° in flexion, 0.14° in extension, 0.63° in right lateral bending and 0.22° in right axial rotation.

Biomechanical behaviours of the lumbar spine with the Coflex model, the Coflex rivet model and the pedicle screw fixation model were compared with those of the intact model. Data were normalised with respect to the intact model as the percentage values under each loading condition.

Table 1. Intervertebral ROM and applied moment among the intact, defect and implantation models under the hybrid test method.

Model	ROM (°)				Total lumbar ROM (°) (L1–L5)	Moment (Nm)
	L1–L2	L2–L3	L3–L4	L4–L5		
Flexion						
Intact	3.66	3.78	3.82	5.11	16.37	10
Defect	3.62	3.75	4.32	5.05	16.74	10
Coflex	3.49	3.63	4.14	4.84	16.10	10
Coflex rivet	4.33	4.47	1.87	6.01	16.68	12
Pedicle screw fixation	4.51	4.67	1.23	6.31	16.72	13
Extension						
Intact	2.70	2.47	2.30	3.27	10.74	10
Defect	2.37	2.05	3.75	2.61	10.78	8
Coflex	3.36	3.06	0.68	3.89	10.99	14
Coflex rivet	3.36	3.08	0.54	3.92	10.90	14
Pedicle screw fixation	3.24	2.93	0.22	4.11	10.50	13
Lateral bending						
Intact	3.69	3.59	3.67	4.32	15.27	10
Defect	3.69	3.62	3.69	4.33	15.33	10
Coflex	3.72	3.65	3.39	4.34	15.10	10
Coflex rivet	3.78	3.70	3.01	4.43	14.92	10
Pedicle screw fixation	4.41	4.17	1.74	5.23	15.55	13
Axial rotation						
Intact	1.81	1.90	2.23	2.50	8.44	10
Defect	1.83	1.92	2.26	2.52	8.53	10
Coflex	1.80	1.86	2.13	2.53	8.32	10
Coflex rivet	1.80	1.86	2.12	2.53	8.31	10
Pedicle screw fixation	2.17	2.08	1.33	2.79	8.37	13

3. Results

3.1 Range of motion

In extension, the ROM increased by 64% in the defect model at the surgical segment. After implantation, the ROM effectively decreased by 70% in the Coflex model, 76% in the Coflex rivet model and 90% in the pedicle screw fixation model when compared with the intact model (Figure 2). In addition, the ROM increased by 24% in the Coflex and Coflex rivet models at the adjacent L1–L3 segments and increased by 20% at the adjacent L4–L5 segment. The ROM increased by 19% in the pedicle screw fixation model at the adjacent L1–L3 segments and increased by 25% at the adjacent L4–L5 segment.

In flexion, the ROM increased by 13% in the defect model and 8% in the Coflex model at the surgical segment. In contrast to the two above-mentioned models, the ROM decreased by 52% in the Coflex rivet and 68% in the pedicle screw fixation models at the surgical segment. On the other hand, the ROMs of the defect model and the Coflex model were similar to that of the intact model at both the adjacent L1–L3 (deviation within 4%) and L4–L5 segments (deviation within 4%). However, the ROM increased by 17–18% in the Coflex rivet model and 23–24% in the pedicle screw fixation model at both the adjacent L1–L3 and L4–L5 segments.

In lateral bending, the ROM decreased by 8% in the Coflex model, 20% in the Coflex rivet model and 51% in the pedicle screw fixation model at the surgical segment, when compared with that of the intact model. The ROMs of the Coflex and Coflex rivet models were similar to that of the intact model at both the adjacent L1–L3 (1–2%) and L4–L5 segments (1–2%). However, the ROM increased by 16–23% in the pedicle screw fixation model at both adjacent L1–L3 and L4–L5 segments.

In axial rotation, the ROM decreased by 4.3% in the Coflex model, 4.8% in the Coflex rivet model and 40% in the pedicle screw fixation model at the surgical segment, when compared with that of the intact model. The ROMs of the defect, Coflex and Coflex rivet models were similar to that of the intact model at both the adjacent L1–L3 (deviation within 2%) and L4–L5 segments (deviation within 2%). However, in the pedicle screw fixation model, the ROM increased by 20% at the adjacent L1–L2 segment, 10% at the adjacent L2–L3 segment and 14% at the adjacent L4–L5 segment.

3.2 Maximal von mises stress at the disc annulus

In extension, the maximal disc annulus stress decreased by 75% in the Coflex model, 81% in the Coflex rivet model and 79% in the pedicle screw fixation model at the

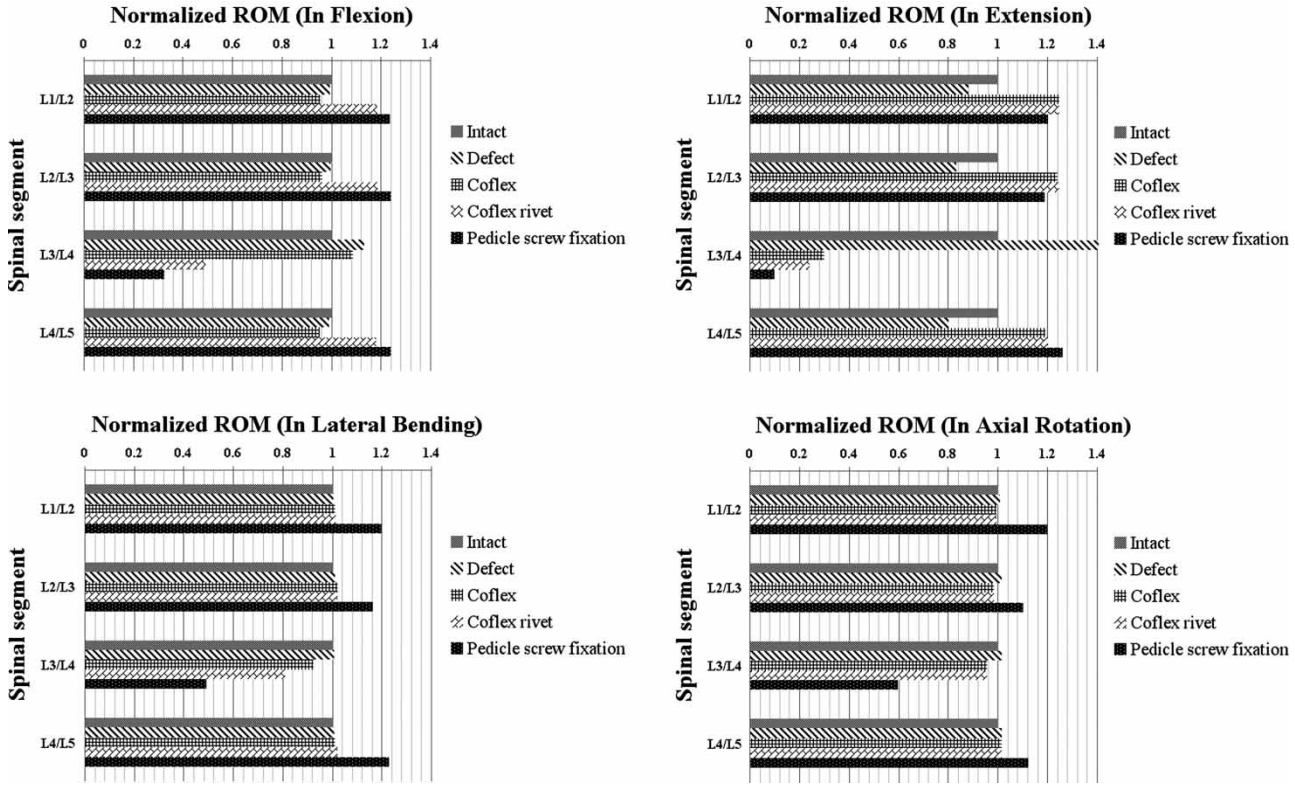

Figure 2. ROM normalised to the intact model in flexion, extension, lateral bending and axial rotation. The Coflex rivet reversed the adverse effects in flexion after Coflex device implantation. The Coflex rivet stabilised all motions in the surgical segment (L3–L4). However, the Coflex rivet affected the adjacent L1–L3 and L4–L5 segments in flexion. In extension, all the interspinous process devices had influence at both the adjacent L1–L3 and L4–L5 segments.

surgical segment when compared with that of the intact model (Figure 3). The maximal disc annulus stress of the Coflex and Coflex rivet models was similar to that of the intact model at the adjacent L1–L2 segment (deviation within 2%). The maximal disc annulus stress of the Coflex and Coflex rivet models increased by 10% at the adjacent L2–L3 segment and decreased by 4% at the adjacent L4–L5 segment. The maximal disc annulus stress of the pedicle screw fixation model increased by 7% at the adjacent L1–L2 segment, 12% at the adjacent L2–L3 segment and 18% at the adjacent L4–L5 segment.

In flexion, the maximal disc annulus stress increased by 5% in the Coflex model at the surgical segment when compared with that of the intact model. In contrast to the Coflex model, the maximal disc annulus stress decreased by 15% in the Coflex rivet and 27% in the pedicle screw fixation models. On the other hand, the maximal disc annulus stress of the Coflex model was similar to that of the intact model at both the adjacent L1–L3 and L4–L5 segments (deviation within 4%). However, the Coflex rivet and pedicle screw fixation models increased maximal disc annulus stress by 18–22% at both the adjacent L1–L3 and L4–L5 segments.

In lateral bending, the maximal disc annulus stress decreased by 18% in the Coflex model, 25% in the Coflex rivet model and 41% in the pedicle screw fixation model at the surgical segment when compared with that of the intact model. The maximal disc annulus stress of the Coflex and Coflex rivet models decreased by 6–8% at both the adjacent L1–L3 and L4–L5 segments. However, the maximal disc annulus stress of the pedicle screw fixation model increased by 15–21% at both the adjacent L1–L3 and L4–L5 segments.

In axial rotation, the maximal disc annulus stress decreased by 15–16% in all the implanted models at the surgical segment when compared with that of the intact model. The maximal disc annulus stress increased by 11% in the Coflex and Coflex rivet models and 7% in the pedicle screw fixation model at the adjacent L1–L2 surgical segment. The maximal disc annulus stress of all the implanted models increased by 15% at the adjacent L2–L3 segment. The maximal disc annulus stress of the Coflex and Coflex rivet models were similar to that of the intact model at the adjacent L4–L5 segment (deviation within 2%). The maximal disc annulus stress of the pedicle screw fixation model increased by 19% at the adjacent L4–L5 segment.

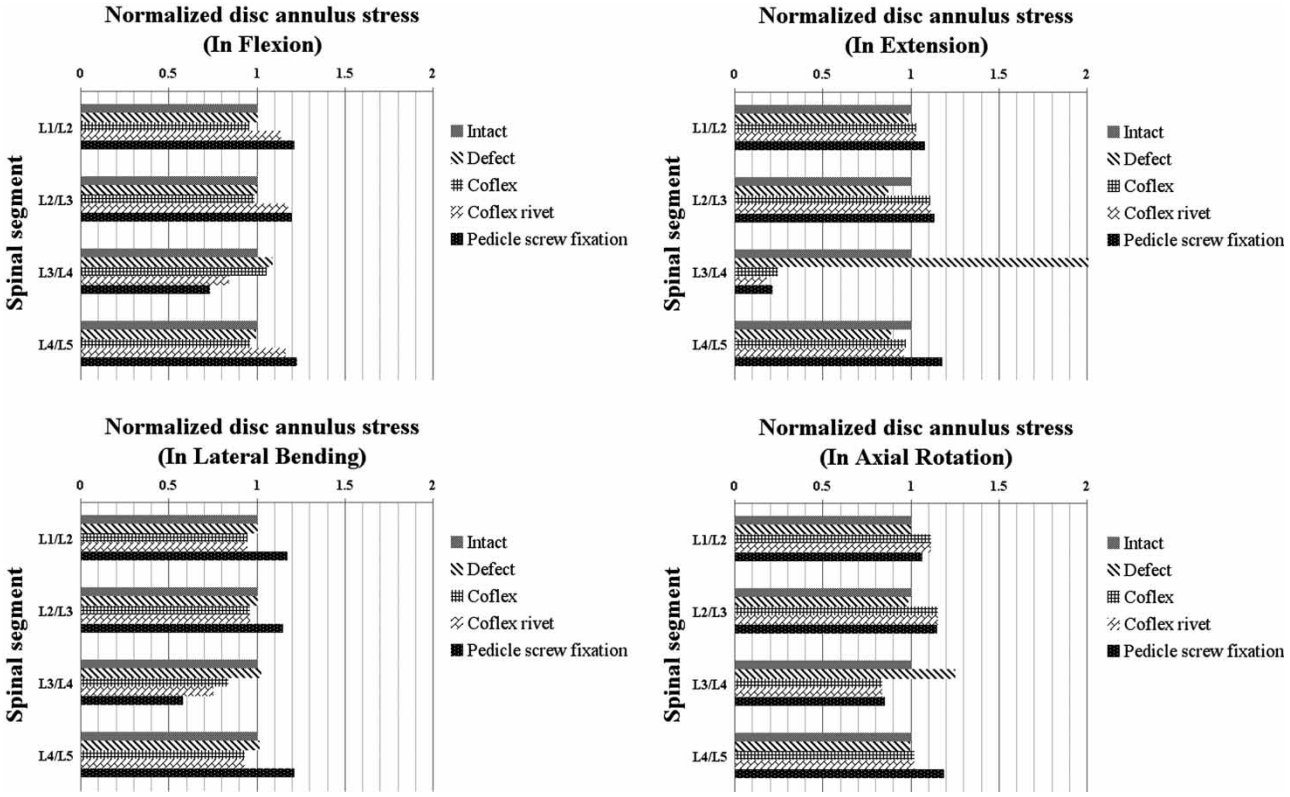

Figure 3. Maximal von Mises stress of the disc annulus normalised to the intact model in flexion, extension, lateral bending and axial rotation. The Coflex device decreased annulus stress at the surgical segment (L3–L4) in extension. However, the Coflex rivet decreased annulus stress at the surgical segment in both flexion and extension.

3.3 Stress distribution of the disc annulus (L3–L4)

Stress concentration and distribution pattern of the disc annulus at the surgical segment changed obviously in these models. In extension, the stress of the defect model was concentrated at the posterior–inferior regions of the annulus (Figure 4). However, after implantation, the stress concentration of the disc annulus at the posterior disc diminished obviously. Furthermore, in flexion, the stress was concentrated at the anterior of the annulus regions, close to the superior and inferior sides of the endplate,

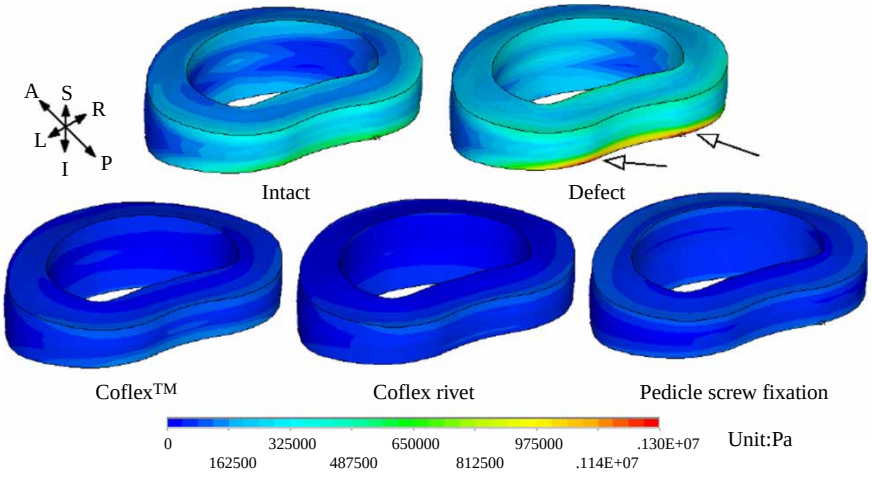

Figure 4. Stress distribution of the surgical segment (L3–L4) disc annulus in extension for various surgical models. The stress of the intact and defect models was concentrated at the posterior–inferior regions of the annulus. After implantation, the stress concentration of the disc annulus diminished obviously.

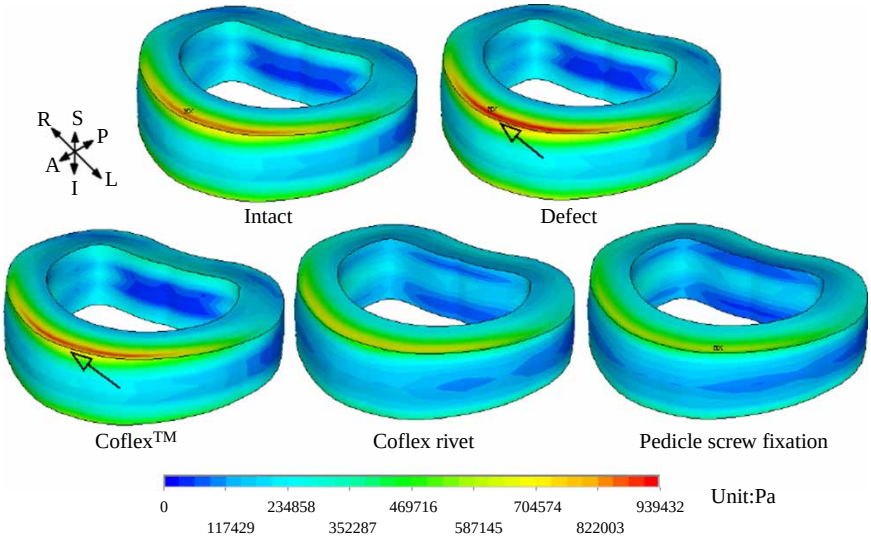

Figure 5. Stress distribution of the surgical segment (L3–L4) disc annulus in flexion for various surgical models. The stress was concentrated at the anterior regions of the annulus, which were close to the superior and inferior sides of the endplate in the defect and Coflex models. The Coflex rivet and pedicle screw fixation models have the most even disc annulus stress distribution.

in both the defect and Coflex models when compared with that of the intact model (Figure 5). The Coflex rivet and pedicle screw fixation models was found to have the most even disc annulus stress distribution in flexion, even when compared with the intact model. In lateral bending and axial rotation, the stress was concentrated at the right part of the annulus regions, close to the superior and inferior sides of the endplate in the defect model when compared with that of the intact model (Figures 6 and 7). After implantation, the stress concentration of the disc annulus at the posterior disc was also diminished.

4. Discussion

The present study found that (1) the Coflex device can provide stability of the surgical segment in most motions, except in flexion; (2) the rivets of the Coflex rivet link bone and implant can provide stability in all motions, especially in flexion; (3) in flexion, the disc stress distribution of the surgical segment is improved by the use of rivets; (4) in flexion, the Coflex rivet increased both ROM and stress of the disc in the adjacent segments and (5) in extension, all implants increased ROM and varied stress of disc in the adjacent segments.

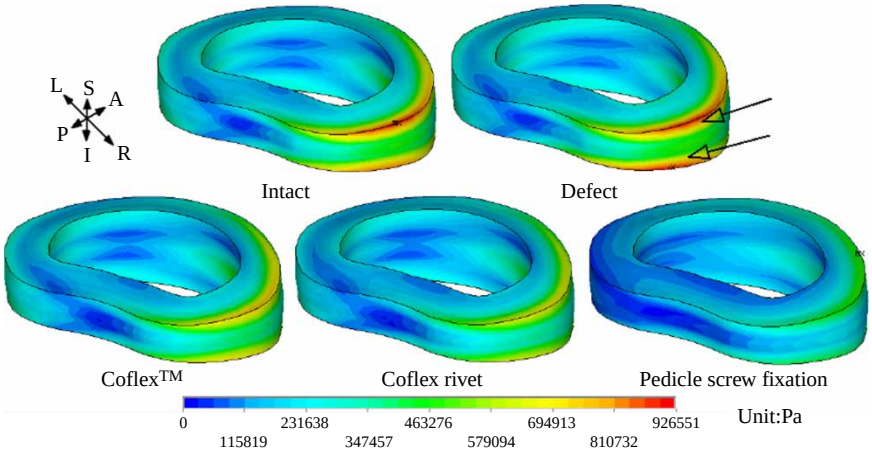

Figure 6. Stress distribution of the surgical segment (L3–L4) disc annulus in right lateral bending for various surgical models. The stress was concentrated at the right regions of the annulus, which were close to the superior and inferior sides of the endplate in the intact and defect models. The Coflex and Coflex rivet models have the most even disc annulus stress distribution. After pedicle screw fixation, the stress concentration of the disc annulus diminished obviously.

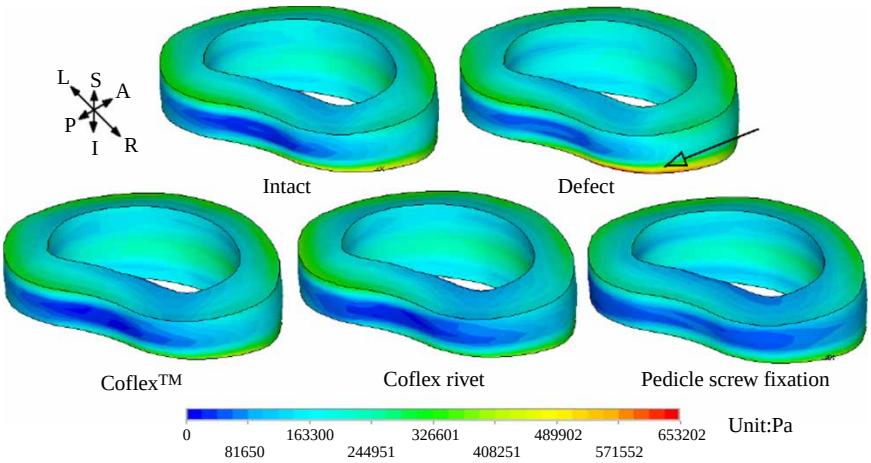

Figure 7. Stress distribution of the surgical segment (L3–L4) disc annulus in right axial rotation for various surgical models. The stress was concentrated at the right regions of the annulus, which were close to the inferior sides of the endplate in the defect model. After implantation, the stress concentration of the disc annulus diminished obviously.

The Coflex devices are primarily used for LSS without degenerative spondylolisthesis, angular instability and retrolisthesis. Only a few reports of *in vitro* flexibility tests of the Coflex device are available in the literature. Among them, results regarding the biomechanical effects of the Coflex device at the surgical segment are inconsistent (Tsai et al. 2006; Kettler et al. 2008; Wilke et al. 2008), especially, the stability in lateral bending and axial rotation. In the present study, the Coflex device in the defect model was found to provide stability in most motions, except in flexion. The instability of the Coflex device in flexion causes stress concentration at the anterior regions of the disc annulus (close to the superior and inferior sides of the endplate). Wilke et al. (2008) suggested that the key for the Coflex device to provide stability in flexion is based on whether the teeth on the wings of the Coflex can provide sufficient anchorage to the spinous process. Two factors can improve this stabilisation effect. First, the surgeon must tighten the teeth on the wings against both the edges of the spinous processes. Second, the bone density of the spinous processes should be strong enough to provide sufficient anchorage. However, both the conditions are not always guaranteed.

For numerical analysis, the coefficient of friction in the interface between the implant and spinous processes was difficult to obtain. It is hypothesised that the teeth on the wings of the Coflex device will prevent implant slip motion in the spinous processes, and therefore, a higher coefficient of friction (0.8) was used in the contact interface. In addition, this study also tested different coefficients of friction (0.4, 0.8, 1.2 and 1.6) to seek its influence on the effect of teeth on the wings of the Coflex device. The results show that the influence of the coefficient of friction is negligible.

The Coflex device was implanted between the interspinous processes located at the posterior structure of the spine to resist instability in extension. In comparison with our previous results in cadaveric experiments (Tsai et al. 2006), our data show discrepancies in lateral bending and axial rotation. It is inferred that these were caused by individual differences among cadaveric specimens and different experimental conditions. In the present study, a partial L3–L4 interspinous process was removed to provide sufficient space for the implant, and the spinous process interface was modelled as a perfect contact and was able to transmit both tensile and compression forces. This assumption is different from that of the cadaveric experiments.

Kettler et al. (2008) reported that implantation of the Coflex rivet can provide stability for all motions in lumbar spine. In the present study, we also showed that the rivet connecting the metal wings and bony spinous process provides more security than the conventional Coflex device. Therefore, the rivet can improve load transmission on the posterior spinal structure to decrease the stress concentration on the disc annulus at the surgical segment in all motions.

There are limited reports about implanting the Coflex device in the long lumbar segment model. The potential side effects in the adjacent segments need to be addressed. In a 1-year outcome evaluation, Kong et al. (2007) reported that the Coflex device reduced the ROM at the surgical segment, but did not affect the ROM at the adjacent segments. The present study, using a long lumbar spine segment model of an implanted Coflex device, showed that the ROMs are increased at both the adjacent segments in extension, but are unchanged in other motions. Therefore, the Coflex device increased annulus stress at both the adjacent segments in extension. However, the Coflex rivet constrained the surgical segment in all motions and it increased ROM at the adjacent segments, especially in flexion. Therefore, the

Coflex rivet increased annulus stress at both the adjacent segments in flexion and extension. The Coflex rivet and pedicle screw fixation have the same effect on the adjacent segments in both flexion and extension. In addition, the remote adjacent L1–L2 and L2–L3 segments demonstrate the same effect in all forms of implantations.

Several limitations in the present study are related to the assumption of simplified and idealised material properties during simulation, such as the linearised behaviour of the spinal ligaments and pure elastic intact discs without degeneration (Chen et al. 2001; Chen et al. 2009; Zhong et al. 2009). The most common cause of LSS is a degenerative disc. Such discs can lead to bulging or protrusion of the intervertebral disc, facet joint hypertrophy and hypertrophy of the ligamentum flavum. Each of these processes reduces the normal space available for nerves to cause LSS. However, it is difficult to grade the quality of a degenerative disc. Therefore, the defect model, we used mimicked that used in previous *in vitro* studies (Tsai et al. 2006; Kettler et al. 2008).

Furthermore, the degree of gripping force applied between the wings of the Coflex device and the spinous process is determined by the clamping force that is applied by the surgeon. The magnitude of the clamping force applied by the surgeon is difficult to measure, and there have been different results presented in previous studies (Tsai et al. 2006; Kettler et al. 2008; Wilke et al. 2008). In addition, determination of gripping force must also consider bone strength and geometry of the spinous process. In this study, determination of the degree of gripping force was simplified and only the friction conditions between the teeth on the wings of the Coflex device and the spinous process were considered. The coefficient of friction used here was based on the results of a previous study on friction parameters between the cage and the bone (Chen et al. 2009). In addition, our simplified simulation of the gripping force ignored the pre-force between the teeth of the wings and the spinous processes, as well as the inward and outward deformation of both side flanks of the Coflex device. The loading conditions in the present FE simulations were similar to those of the traditional *in vitro* tests. Thus, muscle contraction and pelvic movement were not included in the present study. Furthermore, FE models should be interpreted only as a trend because of the variability among different human tissues.

5. Conclusions

The Coflex device implantation can provide stability in extension, lateral bending and axial rotation at the surgical segment, and it had no influence at adjacent segments except during extension. The Coflex rivet implantation can provide stability in all motions and can reconstruct the posterior spinal structure for load sharing to reduce disc annulus stress at the surgical segment. However, the Coflex rivet caused a higher ROM and stress at both adjacent discs and may result in adjacent segment degeneration in flexion and extension.

Acknowledgements

This study was supported by a grant from the National Science Council, Taiwan (NSC 96-2320-B-281-002). The simulations were partly performed at the National Center for High-performance Computing, Taiwan. The authors are indebted to Dr Ding-Shinn Chen (Department of Orthopaedic Surgery, Cathay General Hospital, Taiwan) for clinical suggestions made to the manuscript.

References

Arbit E, Pannullo S. 2001. Lumbar stenosis: a clinical review. Clin Orthop. 384:137–143.

Chen CS, Cheng CK, Liu CL, Lo WH. 2001. Stress analysis of the disc adjacent to interbody fusion in lumbar spine. Med Eng Phys. 23:483–491.

Chen SH, Zhong ZC, Chen CS, Chen WJ, Hung C. 2009. Biomechanical comparison between lumbar disc arthroplasty and fusion. Med Eng Phys. 31(2):244–253.

Cho KS. 2005. Clinical outcome of the Interspinous-U (posterior distraction device) in the elderly lumbar spine. New York: Spinal Arthroplasty Society.

Christie SD, Song JK, Fessler RG. 2005. Dynamic interspinous process technology. Spine. 30(16 Suppl):S73–S78.

Eberlein R, Holzapfel GA, Schulze-Bauer CAJ. 2001. An anisotropic constitutive model for annulus tissue, and enhanced finite element analysis of intact lumbar disc bodies. Comput Methods Biomech Biomed Engin. 4(3): 209–230.

Eif M, Schenke H. 2005. The interspinous-U: indications, experience, and results. New York: Spinal Arthroplasty Society.

Kaech DL, Fernandez C, Lombardi Weber D. 2002. The interspinous "U": a new restabilization device for the lumbar spine. In: Spinal restabilization procedures. Amsterdam: Elsevier Science. p. 355–362.

Kettler A, Drumm J, Heuer F, Haeussler K, Mack C, Claes L, Wilke HJ. 2008. Can a modified interspinous spacer prevent instability in axial rotation and lateral bending? A biomechanical *in vitro* study resulting in a new idea. Clin Biomech (Bristol, Avon). 23(2):242–247.

Kong DS, Kim ES, Eoh W. 2007. One-year outcome evaluation after interspinous implantation for degenerative spinal stenosis with segmental instability. J Korean Med Sci. 22(2):330–335.

Kuslich SD, Danielson G, Dowdle JD, Sherman J, Fredrickson B, Yuan H, Griffith SL. 2000. Four-year follow-up results of lumbar spine arthrodesis using the Bagby and Kuslich lumbar fusion cage. Spine. 25(20):2656–2662.

Lai PL, Chen LH, Niu CC, Fu TS, Chen WJ. 2004. Relation between laminectomy and development of adjacent segment instability after lumbar fusion with pedicle fixation. Spine. 29(22):2527–2532.

Panjabi MM. 2007. Hybrid multidirectional test method to evaluate spinal adjacent-level effects. Clin Biomech (Bristol, Avon). 22(3):257–265.

Panjabi MM, Henderson G, James Y, Timm JP. 2007. StabilimaxNZ) vs. simulated fusion: evaluation of adjacent-level effects. Eur Spine J. 16(12):2159–2165.

Patwardhan AG, Havey RM, Carandang G, Simonds J, Voronov LI, Ghanayem AJ, Meade KP, Gavin TM, Paxinos O. 2003. Effect of compressive follower preload on the flexion–extension response of the human lumbar spine. J Orthop Res. 21(3):540–546.

Polikeit A, Ferguson SJ, Nolte LP, Orr TE. 2003. Factors influencing stresses in the lumbar spine after the insertion of intervertebral cages: finite element analysis. Eur Spine J. 12(4):413–420.

Schmidt H, Heuer F, Simon U, Kettler A, Rohlmann A, Claes L, Wilke HJ. 2006. Application of a new calibration method for a 3D finite element model of a human lumbar annulus fibrosus. Clin Biomech. 21(4):337–344.

Sengupta DK. 2004. Dynamic stabilization devices in the treatment of low back pain. Orthop Clin North Am. 35(1): 43–56.

Tsai KJ, Murakami H, Lowery GL, Hutton WC. 2006. A biomechanical evaluation of an interspinous device (Coflex^{TM}) used to stabilize the lumbar spine. J Surg Orthop Adv. 15(3):167–172.

Vena P, Franzoso G, Gastaldi D, Contro R, Dallolio V. 2005. A finite element model of the L4–L5 spinal motion segment: biomechanical compatibility of an interspinous device. Comput Methods Biomech Biomed Engin. 8(1):7–16.

Wilke HJ, Drumm J, Häussler K, Mack C, Steudel WI, Kettler A. 2008. Biomechanical effect of different lumbar interspinous implants on flexibility and intradiscal pressure. Eur Spine J. 17(8):1049–1056.

Yamamoto I, Panjabi MM, Crisco T, Oxland T. 1989. Three-dimensional movements of the whole lumbar spine and lumbosacral joint. Spine. 14(11):1256–1260.

Zhong ZC, Chen SH, Hung CH. 2009. Load- and displacement-controlled finite element analyses on fusion and non-fusion spinal implants. Proc Inst Mech Eng H. 223(2):143–157.

Zucherman JF, Hsu KY, Hartjen CA, Mehalic TF, Implicito DA, Martin MJ, Johnson DR, II, Skidmore GA, Vessa PP, Dwyer JW, Puccio S, Cauthen JC, Ozuna RM. 2004. A prospective randomized multi-center study for the treatment of lumbar spinal stenosis with the X STOP interspinous implant: 1-year results. Eur Spine J. 13(1): 22–31.